

A simulation study on few parameters of Cherenkov photons in extensive air showers of different primaries incident at various zenith angles over a high altitude observation level

G. S. Das*, P. Hazarika† and U. D. Goswami‡

Department of Physics, Dibrugarh University, Dibrugarh 786 004, Assam, India

We have studied the distribution patterns of lateral density, arrival time and angular position of Cherenkov photons generated in Extensive Air Showers (EASs) initiated by γ -ray, proton and iron primaries incident with various energies and at various zenith angles. This study is the extension of our earlier work [1] to cover a wide energy range of ground based γ -ray astronomy with a wide range of zenith angles ($\leq 40^\circ$) of primary particles, as well as the extension to study the angular distribution patterns of Cherenkov photons in EASs. This type of study is important for distinguishing the γ -ray initiated showers from the hadronic showers in the ground based γ -ray astronomy, where Atmospheric Cherenkov Technique (ACT) is being used. Importantly, such study gives an insight on the nature of γ -ray and hadronic showers in general. In this work, the CORSIKA 6.990 simulation code is used for generation of EASs. Similarly to the case of Ref.[1], this study also revealed that, the lateral density and arrival time distributions of Cherenkov photons vary almost in accordance with the functions: $\rho_{ch}(r) = \rho_0 e^{-\beta r}$ and $t_{ch}(r) = t_0 e^{r/r_\lambda}$ respectively by taking different values of the parameters of functions for the type, energy and zenith angle of the primary particle. The distribution of Cherenkov photon's angular positions with respect to shower axis shows distinctive features depending on the primary type, its energy and the zenith angle. As a whole this distribution pattern for the iron primary is noticeably different from those for γ -ray and proton primaries. The value of the angular position at which the maximum number of Cherenkov photons are concentrated, increases with increase in energy of vertically incident primary, but for inclined primary it lies within a small value ($\leq 1^\circ$) for almost all energies and primary types. No significant difference in the results obtained by using the high energy hadronic interaction models, viz., QGSJETII and EPOS has been observed.

PACS numbers: 95.55.Ka, 98.70.Rz, 41.60.Bq, 91.10.Vr

Keywords: Gamma ray astronomy, Atmospheric Cherenkov technique, CORSIKA simulation

I. INTRODUCTION

The primary objective of the γ -ray astronomy is to detect γ -rays from celestial sources. For this purpose, in the ground based γ -ray astronomy, the Atmospheric Cherenkov Technique (ACT) [2–12] is being used most widely within its operational energy range from around hundred GeV to tens of TeV. This technique is based on detection of Cherenkov photons emitted in the Extensive Air Showers (EASs) that are generated due to the interaction between the primary γ -rays and air nuclei. The γ -ray sources also emit Cosmic Rays (CRs), which are deflected by the intragalactic magnetic fields because of their charge and hence they lose their directional property. Whereas γ -rays, being neutral, they retain their direction of origin. Thus, by the detection of γ -rays one can make an estimate of the positions of those astrophysical objects.

Because of the indirect nature of experiments in ACT as well as due to the presence of huge CR background, a complete Monte Carlo simulation study on atmospheric Cherenkov photons needs to be carried out for the detection of γ -rays with proper estimation of their energy from the observational data of such experiments. It is to be noted that, although both γ -ray and CR can generate EAS, the nature of two are different. EAS generated by γ -ray is purely electromagnetic (EM) in nature, whereas it is an admixture of EM and hadronic cascades in the case of CR. Although many studies have already been done, specially on the lateral density and arrival time distributions of Cherenkov photons in EASs using available simulation techniques [13–17], still it would be a worthy task to have detailed studies on angular distributions as well as on lateral density and arrival time distributions of Cherenkov photons, initiated by γ -ray and hadronic particles, incident at various zenith angles with a wide range of energy, particularly at high altitude observation levels. Keeping this point in mind, in this work we have studied the lateral density, arrival time and angular distributions of Cherenkov photons in EASs at different energies and zenith angles over a high altitude observation level, using two different high energy hadronic interaction models, viz., QGSJETII and EPOS with FLUKA low energy hadronic interaction model available in the CORSIKA simulation package [18]. This is the extension of our earlier work [1] to cover a wide energy range of ground based γ -ray astronomy with a wide range of zenith angles ($\leq 40^\circ$) of primary particles, and to study the angular distribution patterns of Cherenkov photons in EASs.

CORSIKA is a four dimensional detailed Monte Carlo simulation code developed to study the evolution and various properties of EASs in the atmosphere. It can be used to simulate interactions and decays of nuclei, hadrons, muons, electrons and photons in the atmosphere up to energies of the order of 10^{20} eV. For the simulation of hadronic interactions, presently CORSIKA has the option of seven high energy hadronic interaction models and three low energy hadronic interaction models [18]. It uses the EGS4 code [19] for the simulation of EM component of the air shower.

The rest of the paper is organized as follows. In the next section, we discuss about the simulation process involved in this work. The analysis of the simulation work and consequent results are discussed in the Section III. We summarized our work in

* gsdas@dibru.ac.in

† poppyhazarika1@gmail.com

‡ umananda@dibru.ac.in

the Section IV.

II. SIMULATION OF CHERENKOV PHOTONS IN EXTENSIVE AIR SHOWERS

As mentioned in the previous section, we have used the CORSIKA 6.990 simulation package by selecting two high energy hadronic interaction models, viz., QGSJETII.3 and EPOS 1.99 with the low energy hadronic interaction model FLUKA to simulate Cherenkov photons in EAS. In fact, we have generated EASs for the monoenergetic γ -ray, proton and iron primaries incident vertically as well as inclined at zenith angles 10° , 20° , 30° and 40° using the QGSJETII-FLUKA and EPOS-FLUKA hadronic interaction model combinations. The intention to use two different high energy hadronic interaction models in our simulation is to test robustness of conclusions of our work. Moreover, this will also provide an opportunity to compare the performance of the models concerned. QGSJETII is the improved version of the model QGSJET01, which is based on the Gribov-Regge theory [18, 20]. QGSJET is one of the most extensively used high energy hadronic interaction models in the simulation works of CR and γ -ray experiments. On the other hand, EPOS is based on quantum mechanical multiple scattering approach based on partons and strings. The performance of EPOS is better in comparison to RHIC data [21]. In our earlier work [1], we have studied extensively the QGSJET01C, VENUS 4.12 and QGSJETII.3 along with all hadronic interaction models at low energy presently available in CORSIKA. Using the above cited model combinations, the following numbers of showers are generated at different energies and zenith angles for the γ -ray, proton and iron primaries as given in the Table I.

TABLE I: Number of showers generated at different energies for the γ -ray, proton and iron primaries incident at 0° , 10° , 20° , 30° and 40° zenith angles.

Primary particle	Energy	Number of Showers
γ -ray	100 GeV	10,000
	250 GeV	7000
	500 GeV	5000
	1 TeV	2000
	2 TeV	1000
	5 TeV	400
Proton	250 GeV	10,000
	500 GeV	8000
	1 TeV	5000
	2 TeV	2000
	5 TeV	800
Iron	1 TeV	50,000
	5 TeV	4000
	10 TeV	2000
	50 TeV	1000
	100 TeV	600

The energy range of the primaries selected here lies within the typical range of ACT energy for different primaries on the basis of their equivalent number of Cherenkov photon yields. The generation of these showers is done by taking the altitude of HAGAR experiment at Hanle (longitude: $78^\circ 57' 51''$ E, latitude: $32^\circ 46' 46''$ N, altitude: 4270 m) as the observational level. However, few other showers are generated at altitudes of 1000 m and 2000 m with same longitude and latitude as Hanle to study the effect of altitude on nature of EASs. The cores of the EASs are considered to coincide with the centre of the detector array. The geometry of the detector system is taken as a flat horizontal detector array, having 25 non-imaging telescopes in the E–W direction with a separation of 25 m in between two consecutive detectors and also 25 such telescopes in the N–S direction with a separation of 20 m. Each telescope is considered to have 9 m^2 mirror area. To detect a TeV EAS with a large zenith angle, a very wide array of detectors is required for the case of non-imaging detection. Considering the range of energies and zenith angles of our simulated showers, the detector array taken here is quite sufficient for the purpose of this simulation work. In case of the longitudinal Cherenkov photon distribution, photons are counted in the step where they are emitted and for simplicity of calculation it is chosen that their emission angle is wavelength independent. The wavelength window for the Cherenkov photon production is selected as 200 – 650 nm as the wavelength sensitivity of usual photomultiplier tube (PMT) used in ACT lies well within this range. Hence only photons produced by the secondary charged particles within this specified wavelength range are allowed to propagate to the observation level. The absorption and scattering of Cherenkov photons in the atmosphere are not taken into account [18], although there are possibilities that Cherenkov photons may undergo Compton scattering, pair production as well as photoelectric/photoneuclear reactions in the atmosphere. The variable bunch size option of Cherenkov photon is set to "5". This slightly high value of the variable bunch size is used to reduce the size of the simulated data. The parameter STEPC in EGS4 code [19] decides the multiple scattering length for e^- and e^+ , which is set to 0.1. The low energy cutoffs of kinetic energy for hadrons, muons, electrons and photons are chosen as 3.0 GeV, 3.0 GeV, 0.003 GeV and 0.003 GeV respectively. The last two options will help to reduce the shower production time without affecting the final expected outcome. The Linsley's parametrized US standard atmosphere [22] has been used out of the different atmospheric models available in CORSIKA.

III. ANALYSIS OF SIMULATED DATA AND RESULTS

To calculate the lateral density of Cherenkov photons, we have counted the number of photons incident on each detector per shower. The arrival time of a Cherenkov photon over a detector is obtained by calculating the time taken by the photon to reach the detector with respect to the first photon of the shower hitting the array. There are several photons hitting each detector per shower. So, average of their arrival times is calculated for each detector. Moreover, there are fluctuations in Cherenkov photon density and arrival time over each detector from shower to shower. Hence, the variation of Cherenkov photon density and arrival time with respect to core distance is found by calculating their average values for the specified number of showers. These fluctuations of photon density and arrival time as a function of core distance (or for each detector) are expressed by calculating the ratio of their r.m.s to mean values. Averaged over the azimuth, the number of photons produced per angular bin of photon's angular position (with respect to the shower axis) is counted to get angular distribution of Cherenkov photons. Furthermore, to investigate the model dependent variation of any parameter, as in the case of our earlier work [1] we have calculated the percentage relative deviation between the two models for a particular parameter by using the following formula:

$$\Delta_{\chi} = \frac{\chi_{mp} - \chi_{rp}}{\chi_{rp}} \times 100\%. \quad (1)$$

Here Δ_{χ} , χ_{rp} and χ_{mp} represent the relative deviation in percentage of a parameter, the reference model parameter and the given model parameter respectively.

For such analysis of the simulated data, C++ programs have been developed in the platform of the ROOT software [23]. The ROOT software is being developed in CERN for the purpose of the effective handling of huge data of high energy physics experiments. In the following subsections, various aspects of Cherenkov photons' distribution in terms of their lateral density, arrival time and angular position as well as their model dependent features are discussed.

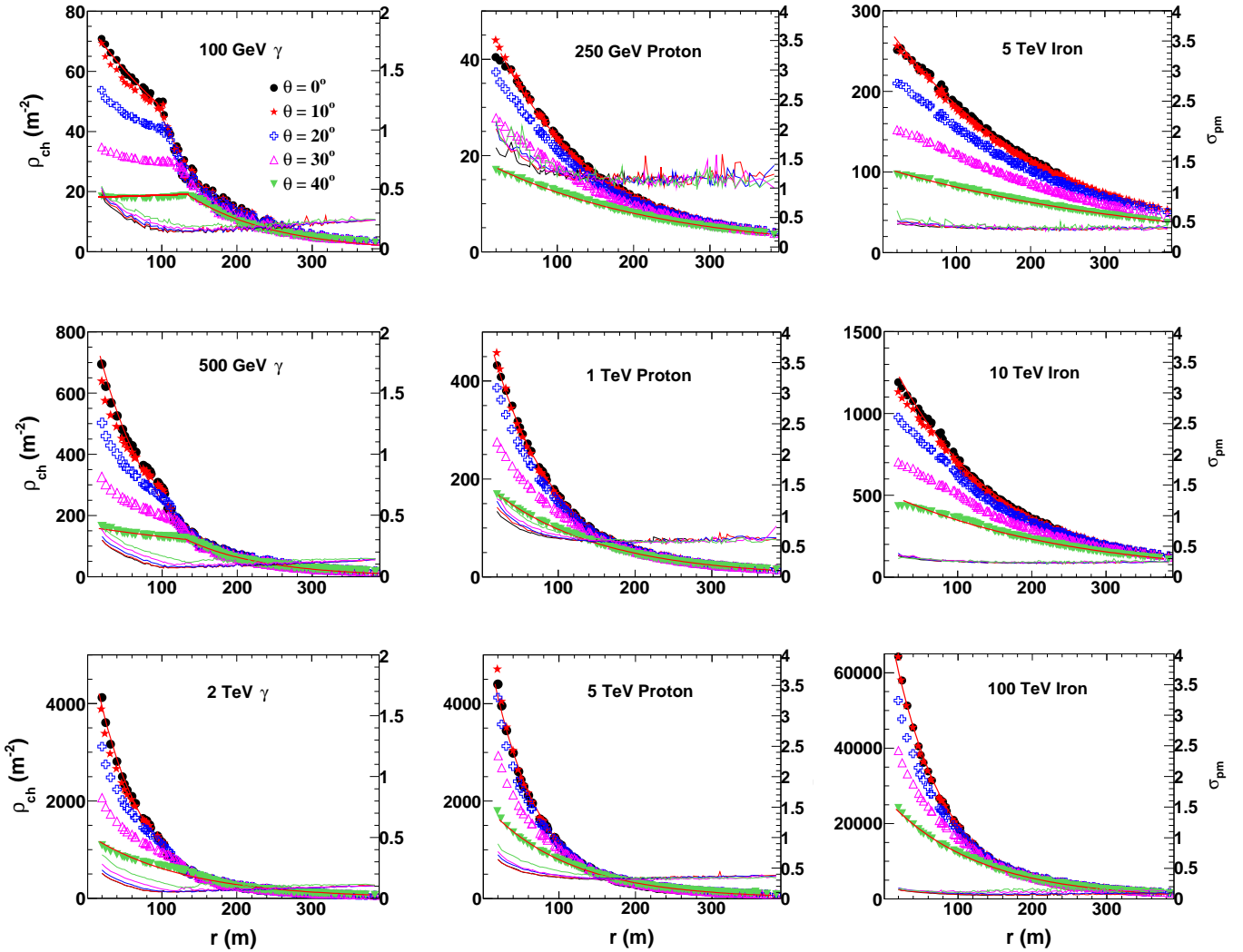


FIG. 1: Average density of Cherenkov photons (ρ_{ch}) and the ratio of r.m.s. to mean of the photon density (σ_{pm}) are plotted with respect to the shower core distance of γ -ray, proton and iron primaries for different energy and angle of incidence. The scale on the right hand side y-axis (y2-axis) is used to read the plots of σ_{pm} . The results of the best fit function (2) are shown by the solid lines in respective plots. The fit on the plots on both sides of the position of hump (wherever is applicable) can be made with the same function with different function parameters.

A. Lateral density of Cherenkov photon

1. General characteristics

Fig.1 shows the variation of average density of Cherenkov photons (ρ_{ch}) and the ratio of r.m.s. to mean of the photon density (σ_{pm}) as a function of the distance from shower core of γ -ray, proton and iron primaries with different energy and at different angle of incidence for the EPOS-FLUKA model combination. To save space, in this figure we have shown the plots only at three different energies for all three primaries, viz. for γ , proton and iron primaries incident vertically as well as inclined at zenith angles 10° , 20° , 30° and 40° respectively. From the figure it is clear that, the ρ_{ch} distribution with core distance falls almost exponentially for all primary particles and their energies with gradual reduction in the slope with increasing zenith angle. The variation in Cherenkov photon density with respect to core distance may be effectively represented by the equation [1]

$$\rho_{ch}(r) = \rho_0 e^{-\beta r}, \quad (2)$$

where $\rho_{ch}(r)$ is the density of Cherenkov photons as a function of position, r is the shower core distance, ρ_0 is the Cherenkov photon's density at the core of a shower and β is the slope. Different primaries will have different values of ρ_0 and β depending upon their energy and the zenith angle. The best fit negative exponential functions, represented by the equation (2), for the vertically incident and also for the most inclined (i.e. incident at 40°) showers are shown by the solid lines in the plots of the Fig.1 as an example. For these fittings we used the χ^2 -minimization method available in the ROOT software [23]. It should be noted that, due to the presence of the significant characteristic hump, the fit for 100 GeV γ -ray primary is made at two segments, one before the position of hump and other after the position of hump with different function parameters. This technique is applied to any plot wherever is required. For the vertically incident primary, this hump is observed at around 100 m core distance. With increasing zenith angle (θ), the distance of the hump from the core increases with increasing prominence, even the hump is seen up to the energy of 1 TeV for the $\theta = 40^\circ$. The geometry of the ρ_{ch} distribution is different for different primary at a particular energy and at a particular angle θ even though the distributions follow the same mathematical function almost for all the cases with different coefficients and slopes. It is observed that for the γ -ray primary at a given energy and θ , the distribution has a larger curvature (beyond the position of the hump along the core distance, wherever applicable) with higher values of the coefficient ρ_0 and slope β of the exponential function (2) in comparison to proton and iron primaries. Moreover, we found that β is smaller for iron primary than that for proton, i.e. for the primary particle of higher mass composition the curvature is smaller.

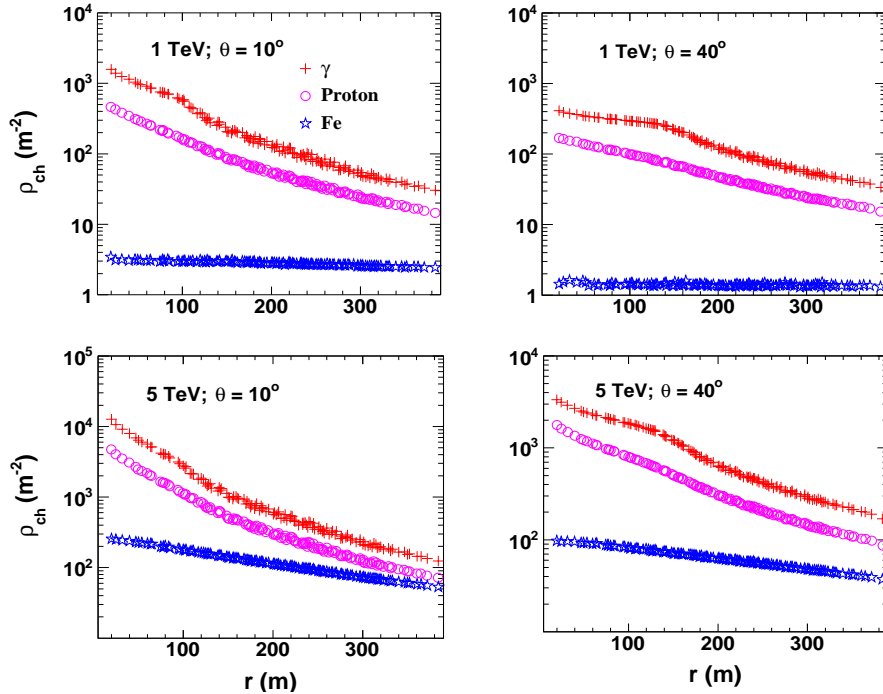


FIG. 2: Distributions of ρ_{ch} with respect to core distance of the showers of γ , proton and iron primaries at 1 TeV and 5 TeV energies incident at 10° and 40° zenith angles.

2. Primary particle and energy dependence

It is quite obvious that the γ -ray primary generates maximum number of Cherenkov photons, whereas the Cherenkov photon yield of iron primary is the lowest at a given energy and zenith angle. This is basically due to the fact that almost whole energy of the γ -ray primary are utilized in the formation of EM shower, whereas in the cases of proton and iron primaries a portion

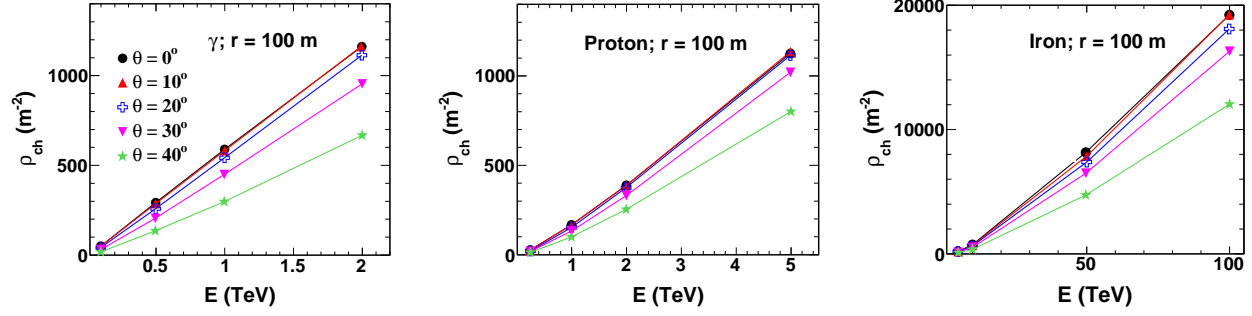


FIG. 3: ρ_{ch} as a function of energy of the primary particle at 100 m distance from the core of the showers of γ , proton and iron primaries.

of their energy is used up in the formation of hadronic shower along with the EM one. Another contributing factor for such behaviour of iron primary is the height of shower maximum. At a given energy and zenith angle, the shower maximum of the iron primary is produced at sufficiently high altitude in comparison to that for the γ -ray and proton primaries. For the γ -ray and proton, this height is nearly equal for the same condition (see the Table II). So, a considerable fraction of EM charged particles (which are sources of Cherenkov photons) of iron initiated shower may be absorbed in the atmosphere before reaching the level of the shower maximum of γ -ray and proton primaries of same energy and zenith angle. In Fig.2, the distributions of ρ_{ch} with respect to the distance of the shower core produced by the γ -ray, proton and iron primaries with 1 TeV and 5 TeV energies and inclined at 10° and 40° are shown to visualize this observation.

Fig.3 shows the variation of ρ_{ch} at 100 m core distance with respect to energy for primary particle of all types. It has been found that, the ρ_{ch} increases at a faster rate, and as well as almost linearly with the energy of the γ -ray primary. On the other hand, for the cases of proton and specially of iron primaries, the increasing trend is comparatively slow and also non-linear with respect to the primary energy. These behaviours of primaries with respect to energy can be understood in the light of explanation mentioned above. Moreover, this figure also indicates the result stated above.

TABLE II: Average slant depth corresponding to shower maximum of EASs produced by γ -ray, proton and iron primaries incident with different energies and at different zenith angles.

Primary particle	Energy	Zenith angle	Shower maximum position (gm/cm ²)
γ -ray	100 GeV	0°	255.856
	500 GeV	0°	313.383
	1 TeV	0°	337.019
		20°	314.837
		40°	262.001
Proton	250 GeV	0°	301.220
	1 TeV	0°	340.016
	2 TeV	0°	360.020
		20°	342.191
		40°	284.292
Iron	1 TeV	0°	200.103
	5 TeV	0°	243.849
		20°	231.510
		40°	190.410
	50 TeV	0°	324.214

3. Photon density fluctuations

It is clear from the Fig.1 that the value of σ_{pm} of ρ_{ch} for γ -ray primaries initially decreases with increasing core distance up to a distance of ~ 100 m and then gradually increases. This pattern continues for all energies and for vertical as well as inclined showers. Moreover, the value of σ_{pm} is found to become smaller with increase in energy of the primaries. Similar pattern in the variation of σ_{pm} is also observed for proton primaries. In the case of proton, the values are much higher than γ -ray primaries with a decreasing trend with increase in energy of the primary. σ_{pm} decrease with increasing energy for the iron primaries also, however its value is much smaller than that of proton and, unlike proton and γ -ray primaries it remains almost constant for iron primaries with increasing core distance [1]. Furthermore, σ_{pm} is highest for the most inclined shower and lowest for the vertical shower in the cases of all primaries, energies and almost for all core distances. This is due to the reason that, as inclination

increases the shower has to travel gradually longer distance to reach the observation level, which creates increasing statistical fluctuation with increasing absorption of shower particles within the atmosphere.

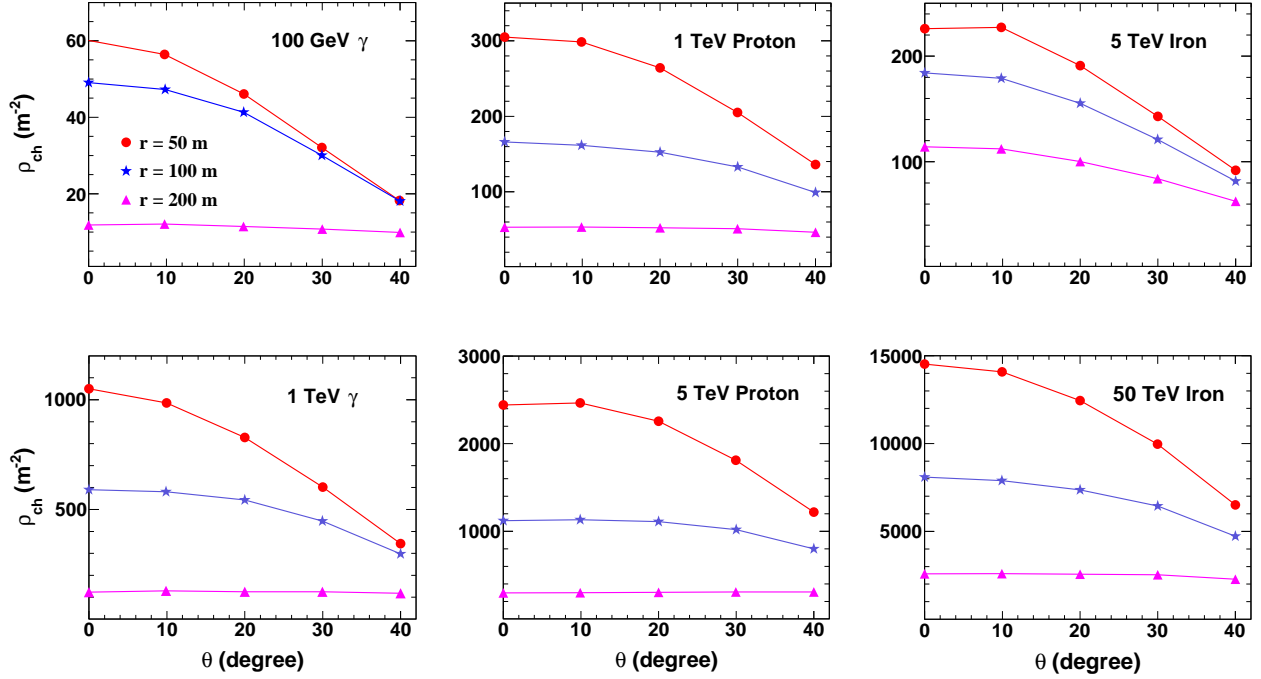


FIG. 4: ρ_{ch} s with respect to zenith angle at 50 m, 100 m and 200 m from the core of the showers of γ , proton and iron primaries.

4. Zenith angle dependence

In Fig.4 the variation of density ρ_{ch} with respect to the zenith angle at distances from the core equal to 50 m, 100 m and 200 m is shown for all the three primaries at two different energies. It is quite clear that up to the distance of 50 m there is very small or no difference in density between vertically incident shower and shower inclined at 10° . Beyond the zenith angle 10° , the density falls off at a faster rate for all combinations of primary particle and energy. At 200 m the variation of density with zenith angle is negligible because only high energetic charged particles, in fact photons from such particles could reach at larger distances from the core over the observation level. At 100 m the pattern of variation of photon density is in between the patterns of variation at 50 m and 200 m. The difference in densities at 50 m and 100 m decreases with increasing angle of incidence, but increases with primary energy. This difference is lowest for γ -ray primaries (in fact zero for 100 GeV γ at 40° zenith angle) and highest for the proton primaries. These observed behaviours of variation of density with the zenith angle is due to the fact that with increasing zenith angle, the (additional) slant depth to be crossed by a shower increases (refer to the Table II) and hence most of the low energy charged particles, i.e. low energy photon's sources get absorbed depending on energy of the primary as well as the nature of generation of shower of the primary itself.

5. Altitude dependence

The density of Cherenkov photons increases with the increasing altitude of the observational level mostly near the shower core ($< r_{hm}$, r_{hm} is the minimum distance from the shower core at which photon density is almost same for all altitudes) for all primary particles incident at any zenith angle and at any energy as long as the observation level remains below the position of the shower maximum of the given primary particle (see Fig.5). Moreover, the difference in density of photons between low and high altitudes of observation level becomes larger with the increasing value of zenith angle. Also with the increasing value of zenith angle, r_{hm} is shifted away from the shower core. These happen because, with increasing slant depth more and more low energetic particles, which are mostly concentrated near the core of the shower, get absorbed as the shower moves towards the lower observation levels. So at lower observation level and at 40° zenith angle, the characteristic hump, which is observed usually for γ -ray primaries, is seen slightly even for the iron primary as well as for the proton primary.

These effects are most observed in the case of γ -ray primary and least observed in the case of iron primary, since a γ -ray primary only produce the EM cascade, which is mainly responsible for the generation of Cherenkov photons, whereas a proton and an iron primaries produce both EM as well hadronic cascade in different proportion, as mentioned above. Due to subsequent production of secondary charged particles by secondary collisions at lower observational level, the Cherenkov photon's density exceeds that at high altitude observation level at large distances ($> r_{hm}$) from the shower core. This is specially more noticeable

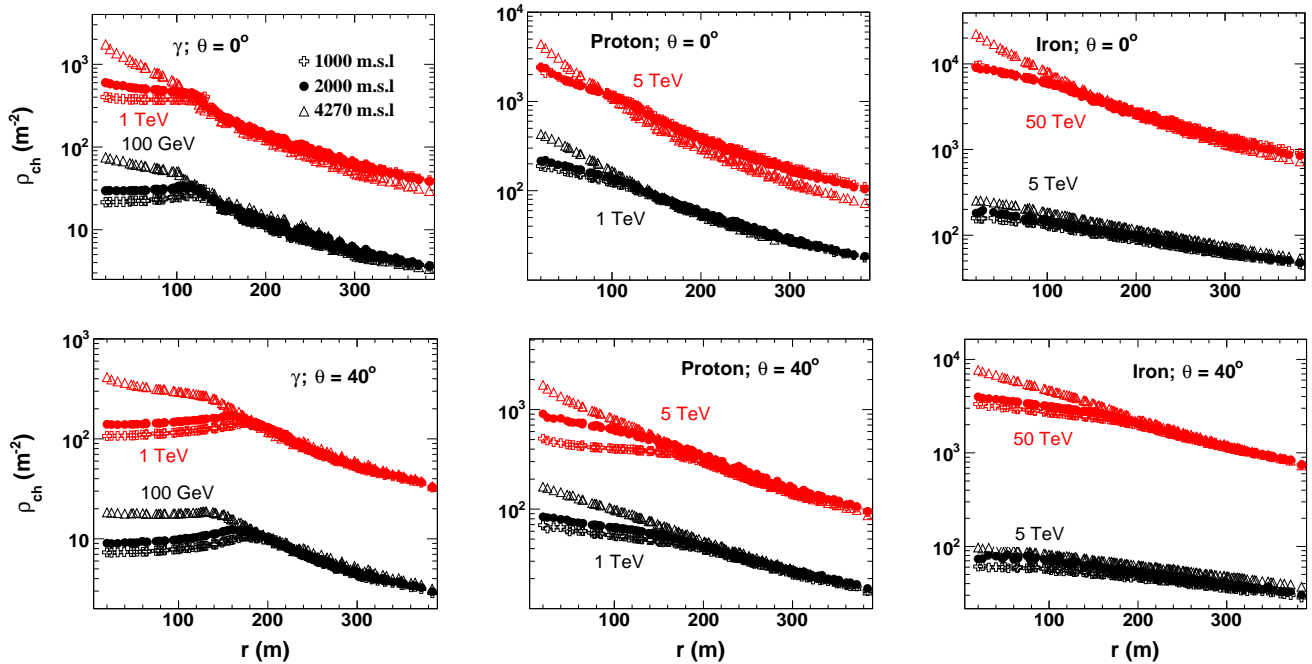


FIG. 5: Variation of ρ_{ch} with distance from shower core at three different altitudes of observation level for γ , proton and iron primary incident at 0° and 40° zenith angles. The black colour is used to represent the low energy plots and the red colour to represent the high energy plots.

for the vertical proton shower at high energy. It should be noted that for the vertical showers of all primary energies, r_{hm} lies in between 100 m to 150 m, whereas for the most inclined shower it lies in between 150 m to 200 m.

6. Hadronic interaction model sensitivity

To see the effect of hadronic interaction models (used in this study) on the lateral density of the Cherenkov photons, the % relative deviation of ρ_{ch} (Δ_ρ) is calculated for the EPOS-FLUKA model combination taking QGSJETII-FLUKA as the reference. Results are shown in the Fig.6 for the vertically incident and 40° inclined showers of different primaries with different energies only as representation. It is to be mentioned that, the reference model combination choice is fully arbitrary, so any one of the two may be used as the reference. For the γ -ray primaries, incident vertically at different energies, there is no considerable differences in densities are seen for these two hadronic interaction model combinations. However, closer to the shower core (< 100 m) some small deviations of $\sim \pm 3\%$ are observed. Beyond this distance the deviations are within $\sim \pm 1\%$. However, for the inclined shower the density deviation is slightly higher (up to $\sim 6\%$), specially at higher energies.

For the proton primary, the deviation between the two models is clearly visible for both vertically incident and inclined showers, and is significant in comparison to γ -ray primary. At lower primary energies these deviations are mostly negative and limited within $\sim 6\%$, while for higher primary energies they are mostly positive. In the case of 1 TeV primary, the deviations are limited to within $\sim -6\%$ to 1% . For the 5 TeV primary with vertical incidence, the deviation extends from $\sim -3\%$ to $\sim 10\%$ and for the inclined shower it ranges from $\sim 2\%$ to $\sim 10\%$.

The deviation in density for the iron primaries are different from the primaries of γ -ray and proton, where the lower primary energy gives higher deviation. At 5 TeV energy, for both vertical and inclined showers, the deviation is maximum ($\sim 13\%$) near the shower core and gradually decreases with distance from the core to match with each other at the farthest points. For 10 TeV primary the deviation is mostly limited within $\sim \pm 3\%$ with the deviation becoming positive from negative near the core. With increasing energy, the deviation for the vertical shower decreases substantially in comparison to inclined shower. For example, at 100 TeV the two models exactly match each other for the vertical shower while for the inclined shower, the deviation is mostly distributed between $\sim \pm 5\%$. To understand this behaviour of the iron primary, the high energy hadronic interaction models QGSJET-II and EPOS shall have to be studied in details carefully.

It is clear that almost all the cases, the deviation is basically high only near the shower core (< 100 m). Also seen that for all primary particles and energies, the density deviation due to these two models is higher for the inclined shower than the vertical shower. However, as a whole on average, the range of deviation is within the acceptable limit ($< \pm 10\%$).

7. Influence of atmospheric model

All our simulations of EASs have been done by using the U.S. standard atmosphere as parameterized by Linsley as mentioned in the previous section. But it is also important to check the influence of different atmospheric models on our results of Cherenkov photon density calculations. For this purpose we have used four different atmospheric models available in CORSIKA

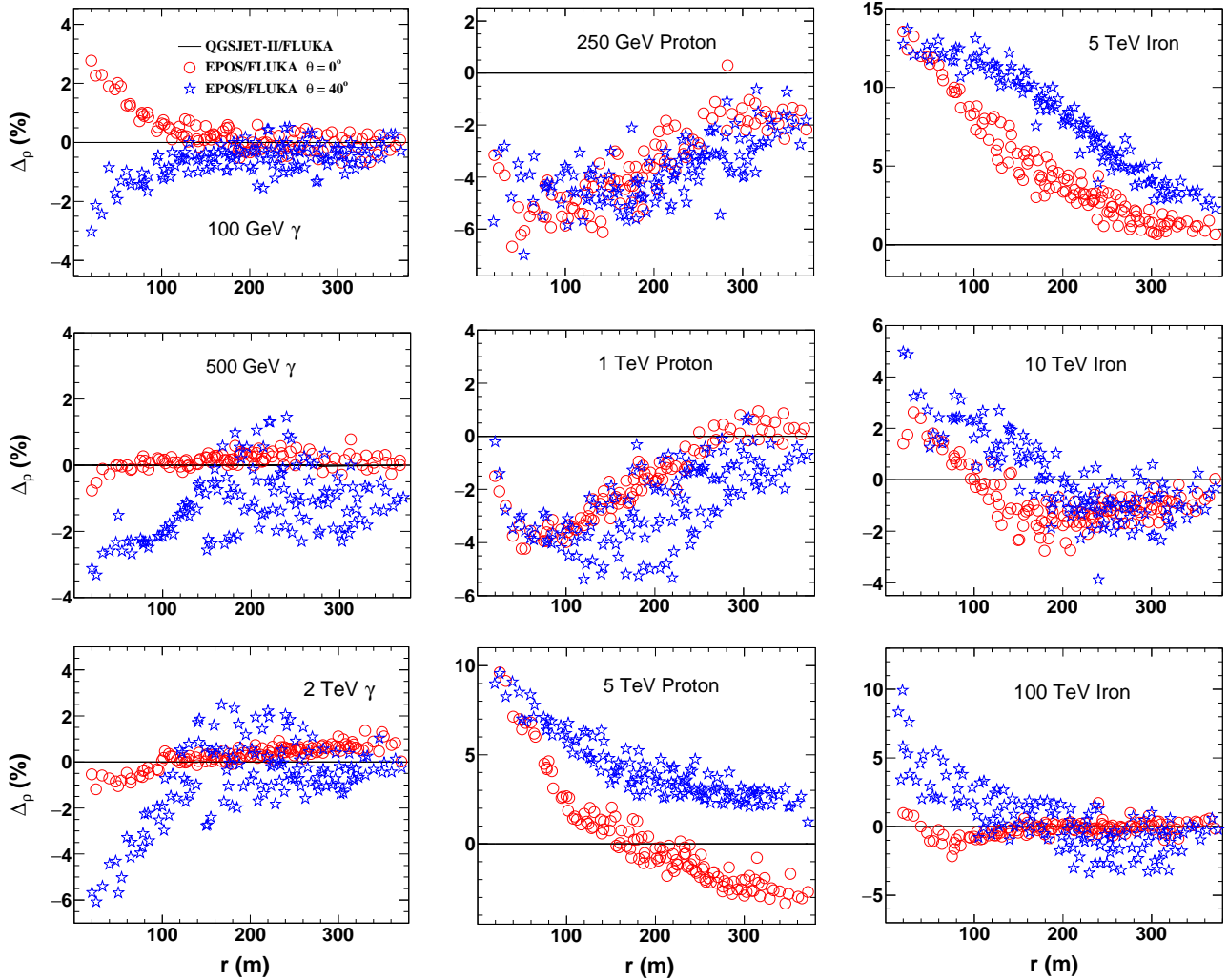


FIG. 6: % Relative deviation of Cherenkov photon densities ($\Delta\rho_s$) with respect to core distance of shower of different primaries obtained by using QGSJETII and EPOS high energy hadronic interaction models at 4270 m altitude of the observation level. The QGSJETII-FLUKA model combination is considered as the reference for the calculation, which is indicated by a horizontal solid line in all plots.

(see the caption of the Fig.7 for detail) by random selection to calculate the Cherenkov photon density for all three primary particles incident vertically at a given energy as shown in the Fig.7. It is found that the difference in densities produced by these atmospheric models are $< 5\%$ for γ -ray, $< 15\%$ for proton and $< 10\%$ for the iron primaries (see the lower panels of the Fig.7). Thus the error that may be introduced in the calculation of Cherenkov photon density due to the use of a particular atmospheric model is found to be small for the γ -ray primary.

B. Cherenkov photon's arrival time

1. General characteristics

The average arrival time of Cherenkov photons (t_{ch}) as a function of core distance has been studied from two perspectives: one with a fixed zenith angle and variable energy, while the other with a fixed energy and five different zenith angles. Some of the results are shown in the Fig.8 and Fig.9 respectively. For all primary particles, energies and zenith angles, the Cherenkov light front is found to be nearly spherical in shape. But, near the shower core (≤ 100 m), t_{ch} increases slowly. The increase of t_{ch} appears to gradually faster with an inconsistent rate as we go away from the core. Because of such inconsistent nature of rate of increase, the distribution deviates slightly from the shape of spherical symmetry. It is clear from the Fig.8 that for all values of zenith angle, the value of t_{ch} increases with increasing energy of the primary. Fig.9 shows that with the increasing angle of incidence the value of t_{ch} decreases for all combinations of energy and primary. The dependence of t_{ch} with the energy and zenith angle of a primary particle can be related with the distance of the detector array from the shower maximum of the particle. With increasing energy of a primary particle this distance decreases (slant depth of the shower maximum increases), whereas it increases (slant depth of the shower maximum decreases) with increasing zenith angle of the particle (see the Table II). Hence above mentioned behaviours of dependence of t_{ch} with the energy and zenith angle of a primary particle are due to respective increase and decrease of number of charged particles of the shower over a detector. Increasing number of charged particles give

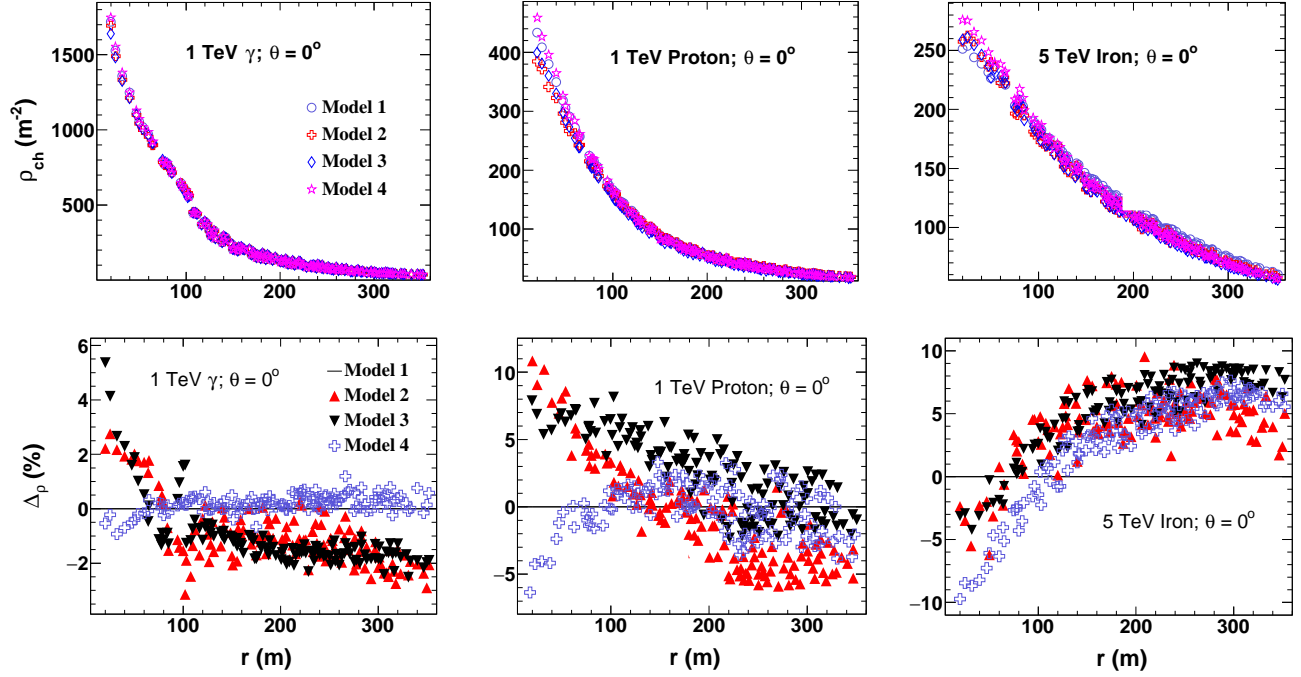


FIG. 7: Variation of ρ_{ch} with distance from the shower cores of γ -ray, proton and iron primaries incident at 0° zenith angle as obtained for four different atmospheric models and the corresponding % relative differences (Δ_ρ) between different model predictions (bottom panels). The Model-1, Model-2, Model-3 and Model-4 represent the U.S. standard atmosphere as parameterized by Linsley, AT 115 Central European atmosphere for Jan. 15, 1993, Malargüe winter atmosphere I after Keilhauer and U.S. standard atmosphere as parameterized by Keilhauer [18] respectively.

increasing time spread of Cherenkov photons produced by a such particles over the detector array and vice verse. Consequently the average arrival time of photons will be increased and decreased. Moreover, it is also evident from these figures that for vertically incident as well for inclined showers the arrival time follows very similar pattern. It is found that for all combinations of energy and zenith angle irrespective of the primary particle, the variation of t_{ch} can be represented by an equation of the form [1]:

$$t_{ch}(r) = t_0 e^{\Gamma/r^\lambda}, \quad (3)$$

where $t_{ch}(r)$ represents the mean arrival time of Cherenkov photons as a function of position, r is the shower core distance. t_0 , Γ and λ are constant parameters. For a given zenith angle, the values of these parameters depend on the type and energy of the primary particle. In the Fig.8 the best fit functions are shown as solid lines for one of the energy corresponding to the different zenith angle. The method used for the fitting is same as that used for the density distributions.

2. Primary particle and energy dependence

In Fig.10 the average arrival time of Cherenkov photons (t_{ch}) with respect to the distance from the shower core is plotted for the three primaries of same energy (in each plot) inclined at 10° and 40° . It is seen that almost in all the cases t_{ch} is higher over all core distances for the γ -ray primary than that for the iron primary, but comparable with that for the proton primary. Hence in general the thickness of Cherenkov photons' light-pool initiated by a γ -ray primary is wider on average than that from the iron primary and is comparable with that for the proton primary of same energy. γ -ray and proton primaries show very similar pattern, but the iron primary initiated photons distinctly have flatter average arrival time.

At a given energy and zenith angle the shower maximum of the iron primary is produced at a significantly higher altitude in comparison to γ -ray and proton primaries. But its value is comparable for the γ -ray and proton primaries (see the table II). Moreover, the nature of production of shower is different for all these three primaries as stated earlier. So, at a given energy and zenith angle, the γ -ray initiated shower takes distinctly longer average time (because of wider time spread) than the iron initiated shower and slightly different average time than the shower of proton primary to reach the observation level. This is due to the reasons explained earlier related with the shower maximum and the nature of shower production.

In Fig.11 we have shown the variation of t_{ch} at 100 m distance from the shower core with respect to energy of the γ -ray, proton and iron primaries incident at various zenith angles. As stated earlier t_{ch} increases with increasing energy of all primary particles due to the decreasing altitude of the position of shower maximum with increasing energy. This increase of t_{ch} is non-linear for the γ -ray (highly) and proton initiated showers, but almost linear for the iron initiated showers. The pattern of increase of t_{ch} for the vertically incident shower of all primaries is almost similar with a slight variation due to the nature of shower production for the primary type.

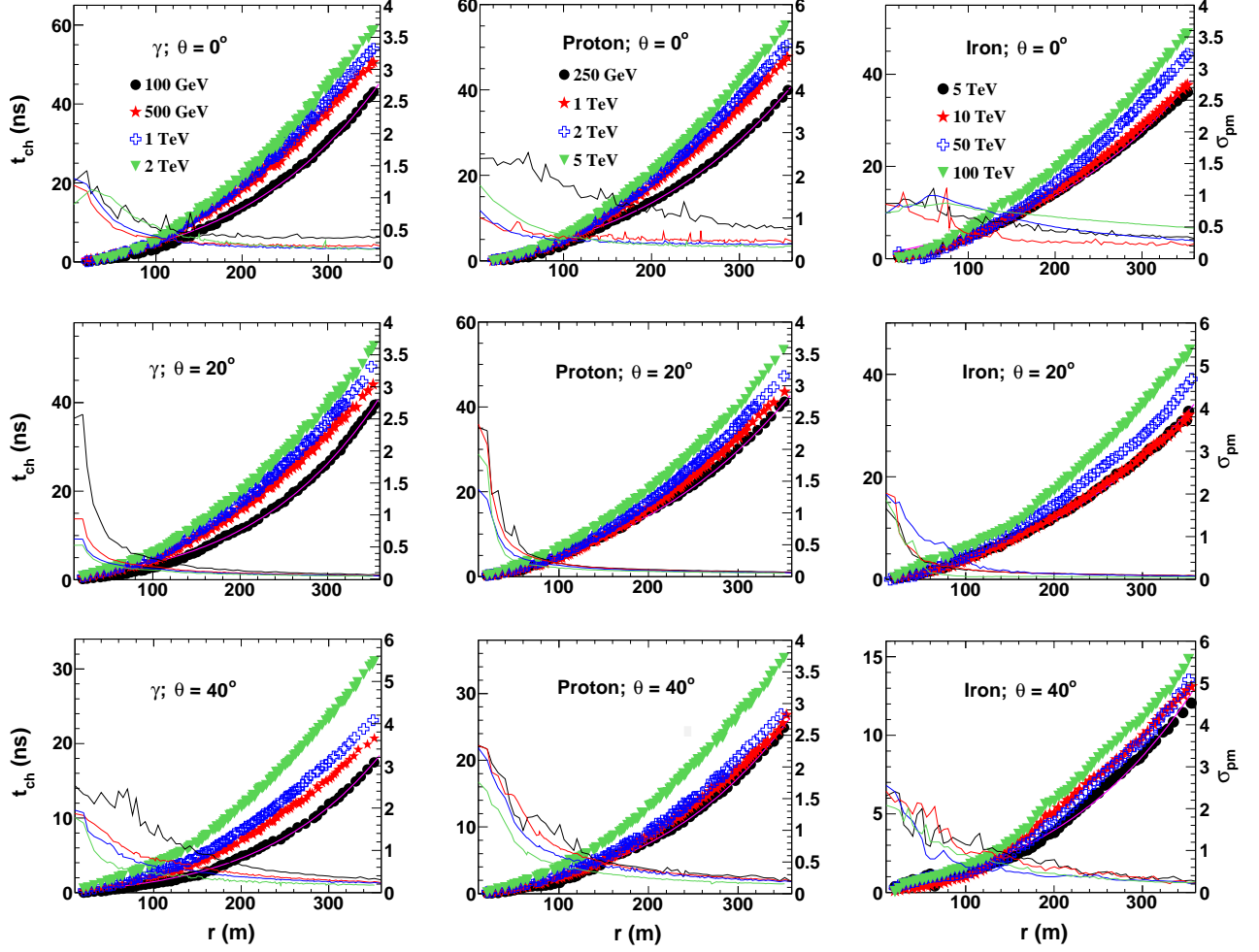


FIG. 8: Average arrival time of Cherenkov photon (t_{ch}) and the ratio of r.m.s. to mean of the photon arrival time (σ_{pm}) as a function of the distance from the core of showers of different primaries with different energies corresponding to some fixed value of zenith angle. The scale on the y2-axis is used to read the plots of σ_{pm} . The solid line in each plot indicates the result of the best fit function (3) into the data for the lowest energy.

3. Photon arrival time fluctuations

We have calculated the ratio of r.m.s. to mean of the photon arrival time (σ_{pm}) for all three primaries having different energy and zenith angle combination, like we did for the density fluctuations. These are plotted in the Fig.8 to see the fluctuations in the t_{ch} distributions. It is clearly visible that, for all showers irrespective of the primary particle, the energy and zenith angle, the fluctuation is large near the shower core but it decreases with increasing distance from the core. On average the proton primary shows maximum fluctuation (highest at 250 GeV) and the iron shows the least. With increasing zenith angle the fluctuations increases further near the shower core with same decreasing pattern with increasing distance. Furthermore, for different primaries σ_{pm} behaves differently. For example, for both γ -ray and proton primaries its value decreases with increasing energy, almost for all core distances and for all zenith angles with slight deviations. But exactly such a behaviour can not be seen for the iron primary.

4. Zenith angle dependence

The variation of t_{ch} with zenith angle for the γ -ray, proton and iron primaries are shown in Fig.12. The figure shows only plots for two different energies of each primary at a core distance of 50 m, 100 m and 200 m. It is observed that, there is an overall falling trend of t_{ch} with respect to zenith angle for all primary particles, energies and at all core distances. This is due to the reason of position of shower maximum in relation to zenith angle as discussed earlier. In the case of γ -ray primaries the trend is most smooth, whereas it is least smooth for the iron primaries. It is because the air shower produced by a γ -ray primary is homogeneous in nature, on the other hand air shower produced by an iron primary is most inhomogeneous. Moreover, with increasing distance from the core of shower, the rate of falling of the t_{ch} increases with the zenith angle. This behaviour is again due to the fact that with the increasing distance of a detector from the shower core, the distance to the shower maximum increases.

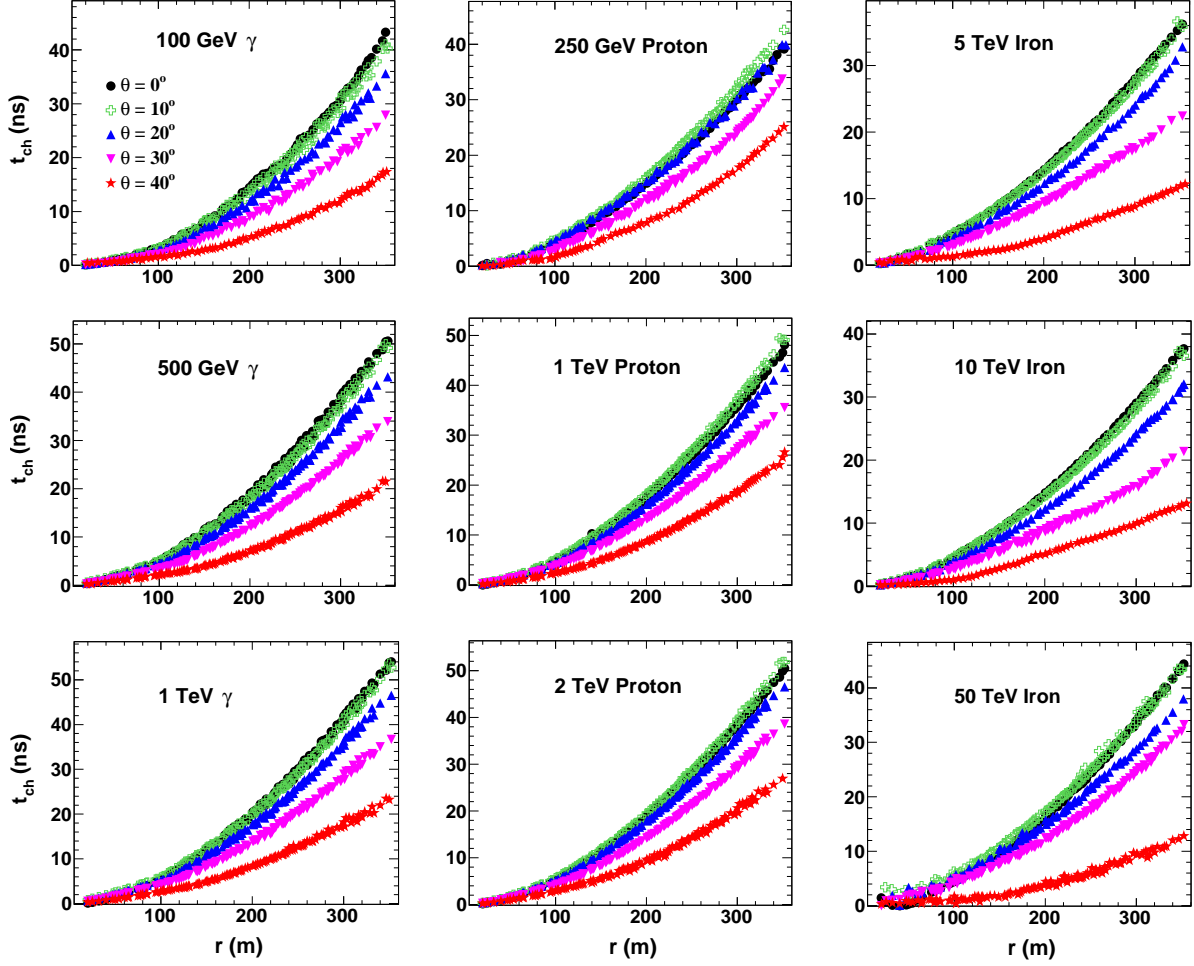


FIG. 9: Average arrival time of Cherenkov photon (t_{ch}) as a function of the shower core distance for different primaries at different zenith angle corresponding to some fixed value of energy.

5. Altitude dependence

With increasing altitude of an observation level, the observation level comes closure to the shower maximum of a shower. Thus for the reason explained earlier, the Cherenkov light front becomes wider with increasing altitude of the observation level and becomes flatter with decreasing altitude (see the Fig.13). This trend will continue if an observation level lies below the position of shower maximum. Similarly for the same reason the arrival time for a inclined shower is found to be shorter in comparison to a vertical shower at a given observation level. These behaviours of arrival time of Cherenkov photons are most prominent for the γ -ray primary and are least prominent for the iron primary for the reason already mentioned in the previous section. Thus the disk thickness [24] of Cherenkon photons at high altitude observation level for a high energy vertically incident primary particle is wider in comparison to that at low altitude observation level and for a low energy primary particle incident with some zenith angle.

6. Hadronic interaction model sensitivity

As in the case of Cherenkov photon density mentioned above, we have studied also the relative deviation in the t_{ch} considering the model combination QGSJETII-FLUKA as the reference model. This is for a better idea about the hadronic interaction model's sensitivity to the Cherenkov photon's arrival time with respect to shower core for different primary particles with different energies and zenith angles. Fig.14 shows the relative deviations in percentage of the arrival times ($\Delta_t s$) of the Cherenkov light fronts obtained from the EPOS-FLUKA and QGSJETII-FLUKA model combinations for various monoenergetic primary particles, incident vertically and at an angle 40° . It is seen that, the deviations in the t_{ch} s due to two the model combinations are small (within $\pm 7\%$) for all the vertically incident as well as inclined primaries. Moreover, for the vertical showers, the difference between the two models is remarkable mainly for the core distances below 100 m, beyond which the % relative variation in t_{ch} is quite small, mostly less than $\pm 3\%$. But for the inclined showers, this difference lies within $\pm 4\%$ to 7% (100 TeV iron) almost throughout the distance from the core.

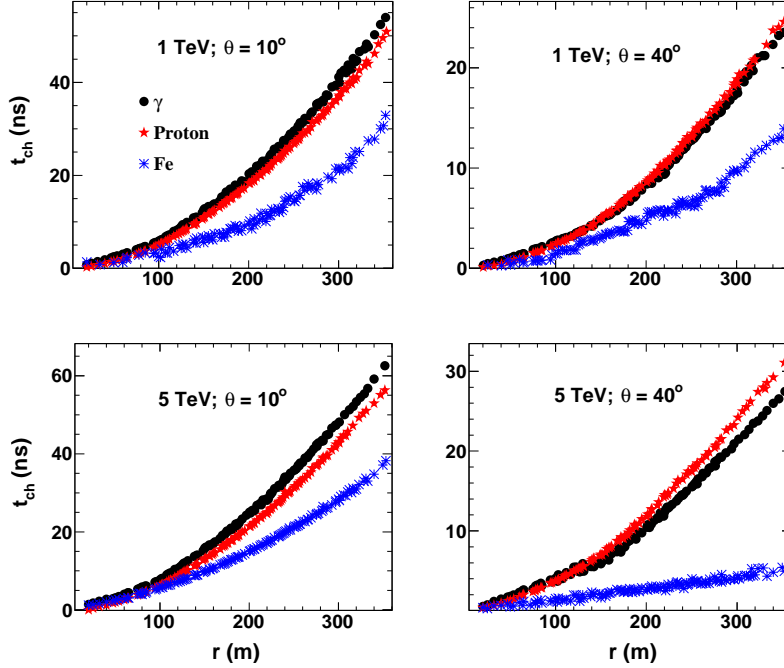


FIG. 10: Variation of t_{ch} with respect to the core distance of the showers of γ , proton and iron primaries of the same energy.

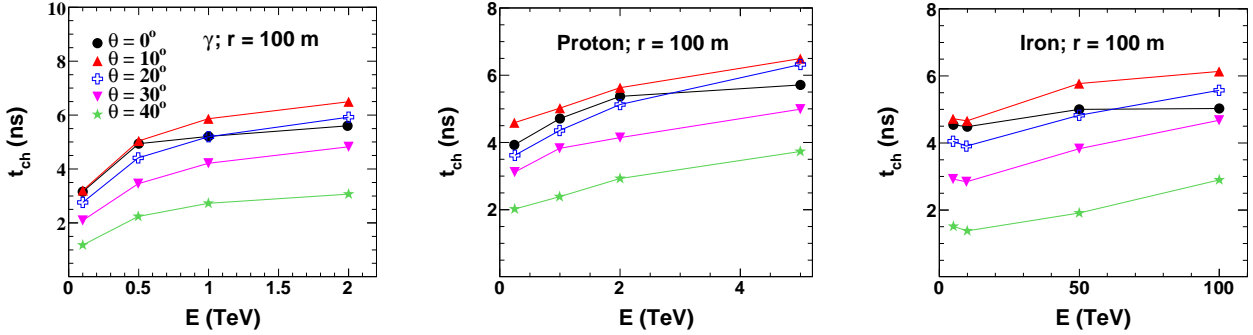


FIG. 11: Variation of t_{ch} as a function of energy of primary at 100 m distance from the shower core of γ , proton and iron primaries.

7. Influence of atmospheric model

Similarly to the case of Cherenkov photon density, we have done the calculation of arrival time of Cherenkov photons using the same atmospheric models to check the influence of atmospheric model consideration in our analysis as shown in the top panels of the Fig.15. It is seen that the difference in arrival times as obtained from these models are $< 10\%$ for the γ -ray, $< 11\%$ for the proton and $< 19\%$ for the iron primaries (see the lower panels of Fig.15). Furthermore, it is observed that for the case of γ -ray primary, only very near the shower core (< 30 m) the deviations go beyond 5%, beyond which the deviations are below 3% only. Hence the effect of the atmospheric model on the calculation of arrival time of Cherenkov photons can be considered negligible.

C. Angular distribution of Cherenkov photons

In this section we study the distribution of Cherenkov photon's average angular position with respect to the axis of a shower of different primary type, energy and zenith angle. The study of this section is basically guided by our theoretical interest rather than experimental implementation point of view. However, this study may provide us an idea to know about the average angular position of photons incident on an imaging detector of IACTs located at a particular distance from the core of a particular shower. On the theoretical aspect, such comparison with experiment with an in-depth view may also help to improve further the high energy hadronic interaction models.

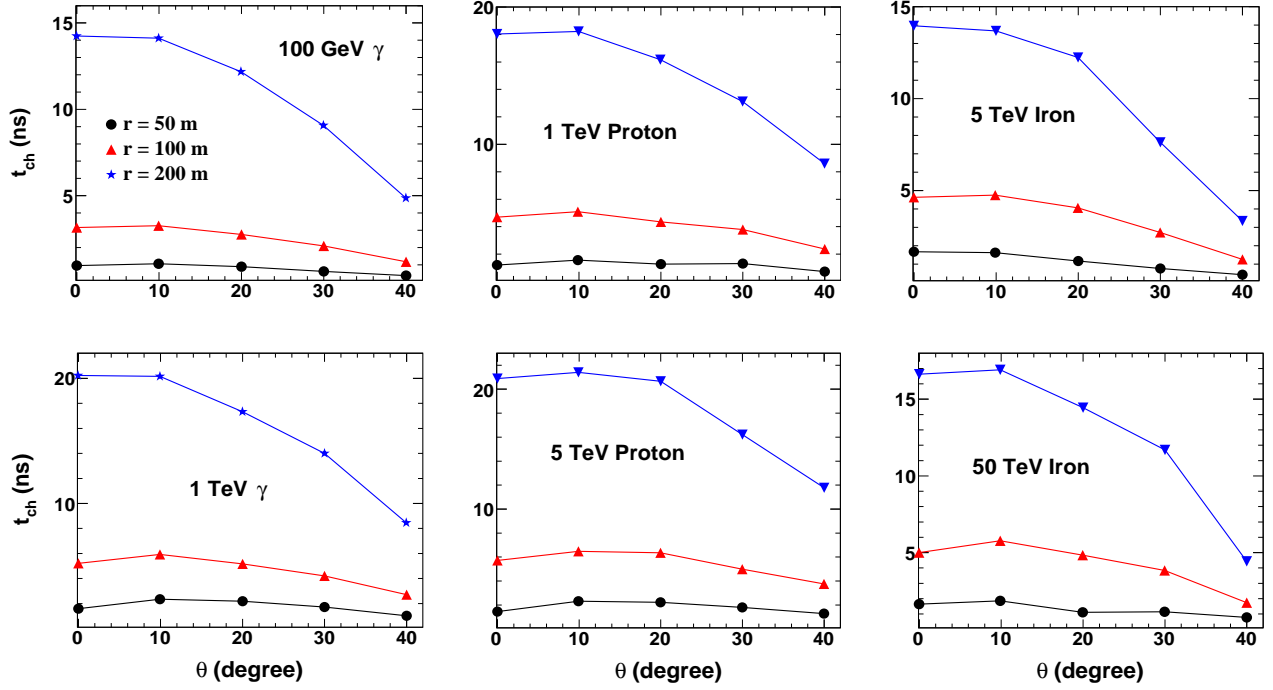


FIG. 12: Variation of t_{ch} with respect to zenith angle at 50 m, 100 m and 200 m from the core of the showers of γ , proton and iron primaries.

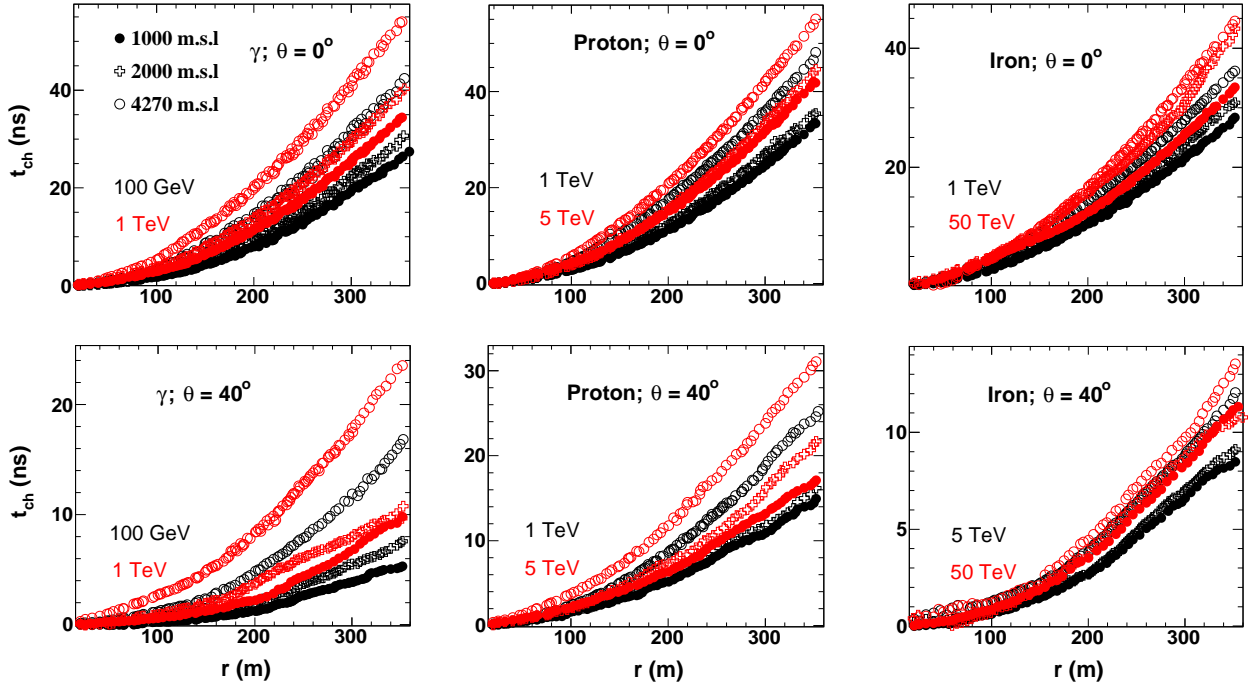


FIG. 13: Variation of t_{ch} with distance from shower core at three different altitudes of observation level for γ , proton and iron primary incident at 0° and 40° zenith angles. Low energy plots are indicated by the black colour, whereas the high energy plots are represented by the red colour.

1. General characteristics

To obtain the angular distribution of Cherenkov photons, the number of photons produced per angular bin ($\frac{dN}{d\alpha}$ (degree $^{-1}$)) of the Cherenkov photon's angular position (α) with respect to the shower axis (see the Fig.16) over each detector are counted. Some of such distributions are shown in the Fig.17 for various combinations of energy and zenith angle for all three primaries. It is seen that the distribution becomes increasingly wider with increase in energy of the primary, specially for the vertically incident particle. With increasing the angle of incidence this tendency decreases gradually and at large incident angle ($> 20^\circ$) it is almost negligible. The first behaviour clearly suggests that, as energy of the vertically incident primary increases, the number of particles deflected at larger angles from the shower core also increases with the proportionate increase in the shower size.

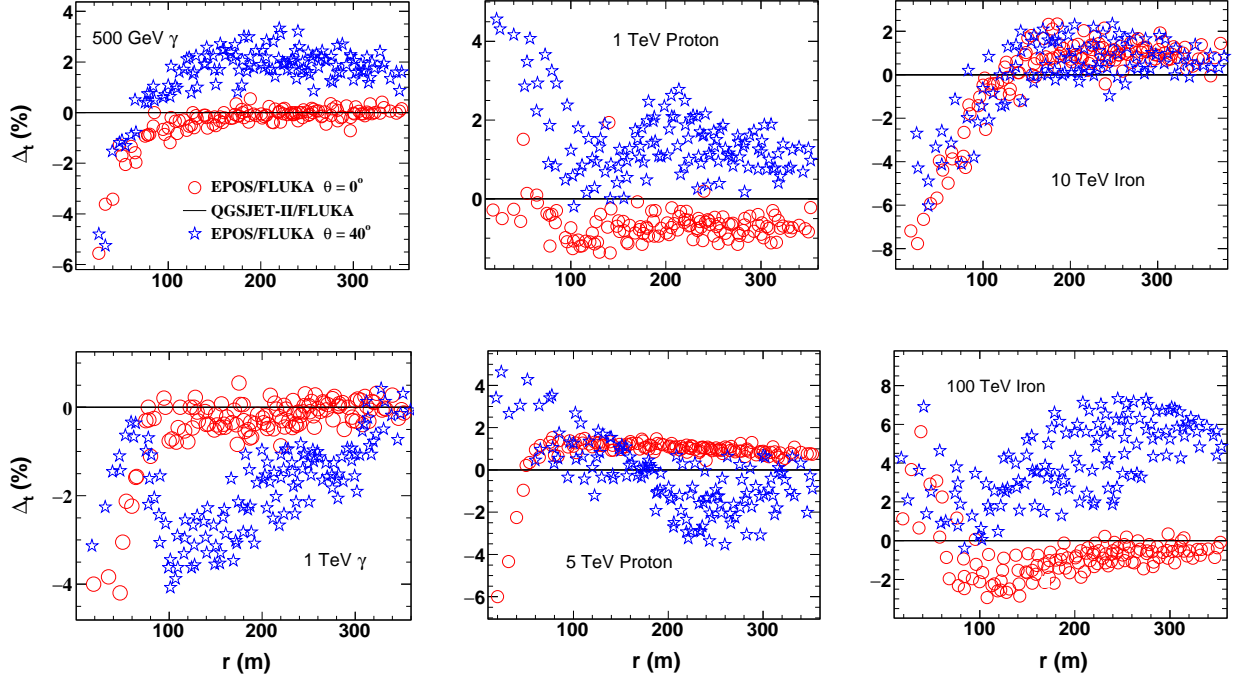


FIG. 14: % Relative deviation of Cherenkov photon's arrival times (Δt s) with respect to core distance of showers of different primaries for the QGSJETII and EPOS models of high energy hadronic interactions. The QGSJETII-FLUKA model combination is indicated by the horizontal solid lines in all plots, which is considered as the reference for the calculation.

Moreover, this tendency of the distribution is most prominent for the γ -ray shower and least prominent for the iron shower. This is because the size of the EM part of a shower (which is deflected most and is responsible for the production of Cherenkov photons) produced by the iron primary is the lowest, whereas the shower produced by γ -ray primary is wholly EM in nature. In addition, it is seen that for the vertically incident showers of all primaries, the value of the angle α at which maximum number of Cherenkov photons are emitted with respect shower axis shifts to higher value with the increasing energy of the primary particle. This shift is highest for the γ -ray primary and least for the iron primary. As discussed in the earlier section, the increase of density of Cherenkov photons with energy is relatively more for the γ -ray primary than that for the proton and specially for the iron primary. So the average value of the angle at which maximum photons are emitted is shifted more towards its higher value for the γ -ray primary than that for proton and iron primaries. Maybe because of the complex nature of the hadron initiated shower, the largest value of α move towards its lower value with the increasing energy of primary particle, specially for the iron (see the top right panel of Fig.17). Similar behaviour can be seen for all primaries incident at larger zenith angle, noticeably for the proton primary in this case. There might be some contributions to these observed behaviours from the height of the shower maximum also, which are different for different primary at a given energy and zenith angle as stated earlier.

It has also been observed that for a particular energy of the primary, the angular distribution profile becomes increasingly narrower as the angle of incidence of primary increases. The reason is as follows. With increasing zenith angle the slant depth of the shower maximum decreases (see the Table II), i.e. shower maximum is produced gradually at higher altitude with increasing zenith angle. Hence, the charged particles of a shower, which emit Cherenkov photons, has to cross gradually longer distance with increasing angle of incidence of the primary particle to reach the observation level. Consequently most of the low energetic as well as highly scattered charged particles are absorbed by the atmosphere before they reach on the observation level. Only sufficiently energetic particles with a smaller angular position α can reach on the observation level depending on the zenith angle of the primary particle, and hence the angular distribution profiles with increasing zenith angles of primary particles become gradually narrower.

Further, the value of α at which maximum photons are emitted with respect to the axis of a shower decreases very slowly with increasing zenith angle. This is also due to the increasing altitude of shower maximum with increasing zenith angle as stated above. Because of the significantly different composition of the iron initiated shower, as mentioned in the previous section, the angular distribution pattern of Cherenkov photons for the iron primary as a whole is quite different that from γ -ray and proton primaries. The distinction between distribution patterns for γ -ray and proton primaries is also noticeable at higher zenith angles.

2. Primary particle, energy and interaction model sensitivity

To see clearly the effect of the type of primary particle on the angular distribution pattern, we have plotted the Cherenkov photon's angular distributions in the showers of γ -ray, proton and iron primaries for two different energies incident at two different zenith angles in the Fig.18. It is seen that at low energy, Cherenkov photons initiated by vertically incident γ -ray are distributed in a small angular range in comparison to the corresponding proton and iron primaries, where iron has the widest

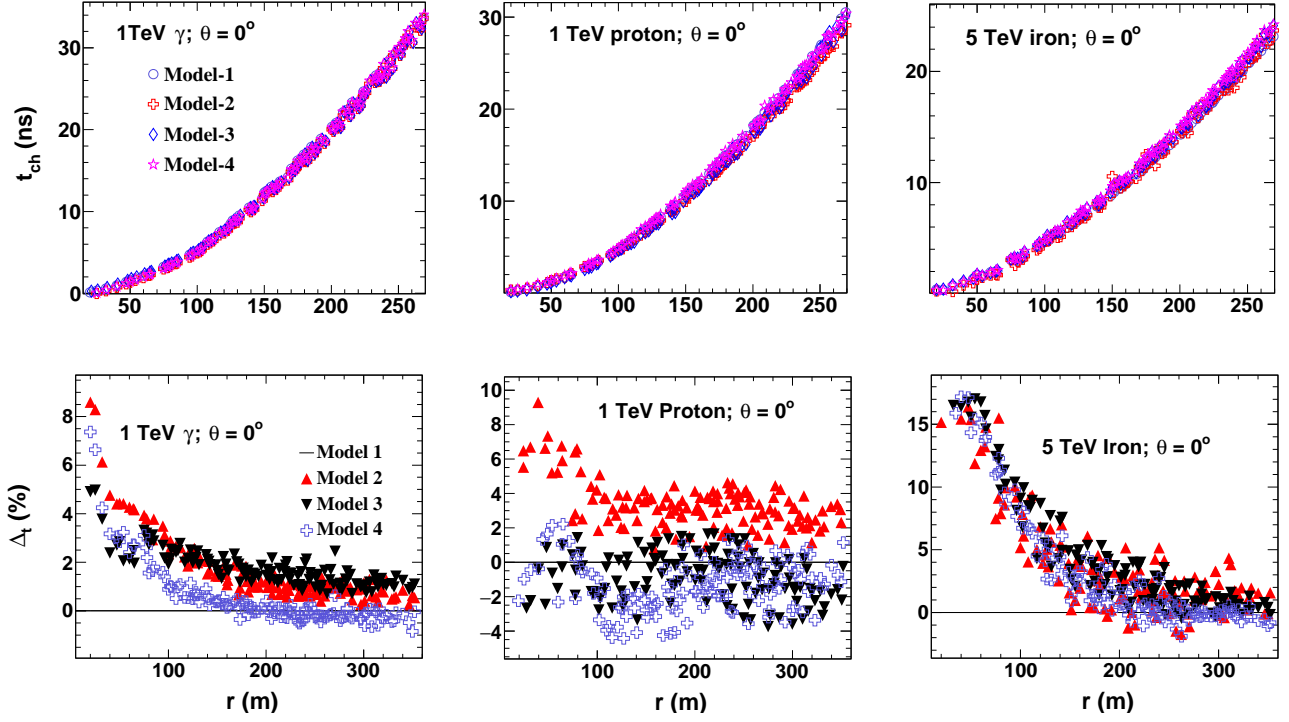


FIG. 15: Variation of t_{ch} with distance from the shower core of γ -ray, proton and iron primary incident at 0° zenith angle as obtained for four different atmospheric models (top panels) and the corresponding % relative differences (Δ_t) between different model predictions. The Model-1, Model-2, Model-3 and Model-4 represent the U.S. standard atmosphere as parameterized by Linsley, AT 115 Central European atmosphere for Jan. 15, 1993, Central European atmosphere for Feb. 23, 1993 and Central European atmosphere for May 11, 1993 [18] respectively.

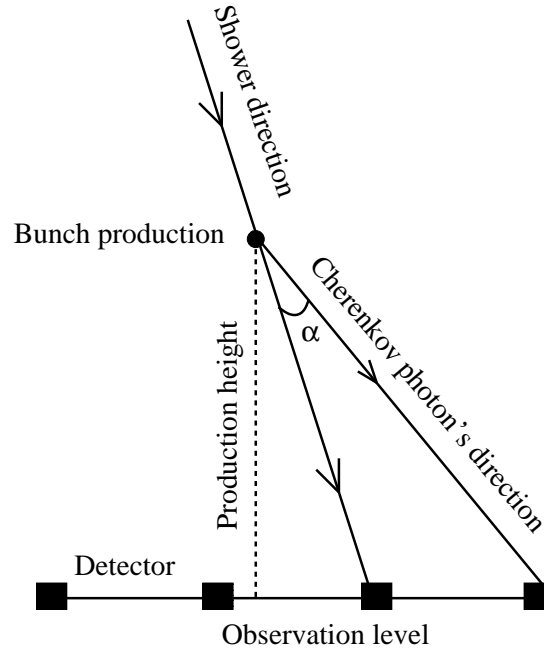


FIG. 16: Schematic of Cherenkov photon's bunch production and the related angular position (α) with respect to the shower axis.

distribution. That is, at low energy the vertically incident iron shower is distributed in a wider range in comparison to proton and γ -ray primaries of same incident angle. But the maximum number of Cherenkov photons are produced very near to shower core similar to the proton. This situation has changed with increase in energy, where iron has the smallest angular range and the proton has the highest. Perhaps, this feature is attributed by the subsequent secondary interactions in the hadronic part of the shower of proton and iron primaries. Moreover, the average angle for the maximum number of Cherenkov photons for the proton primary at higher energy is shifted to comparatively higher side than that for the iron primary of same energy. But this angle is almost same for all three primary types of same energy incident at zenith angles other than zero with additional features related with the zenith angle as discussed above.

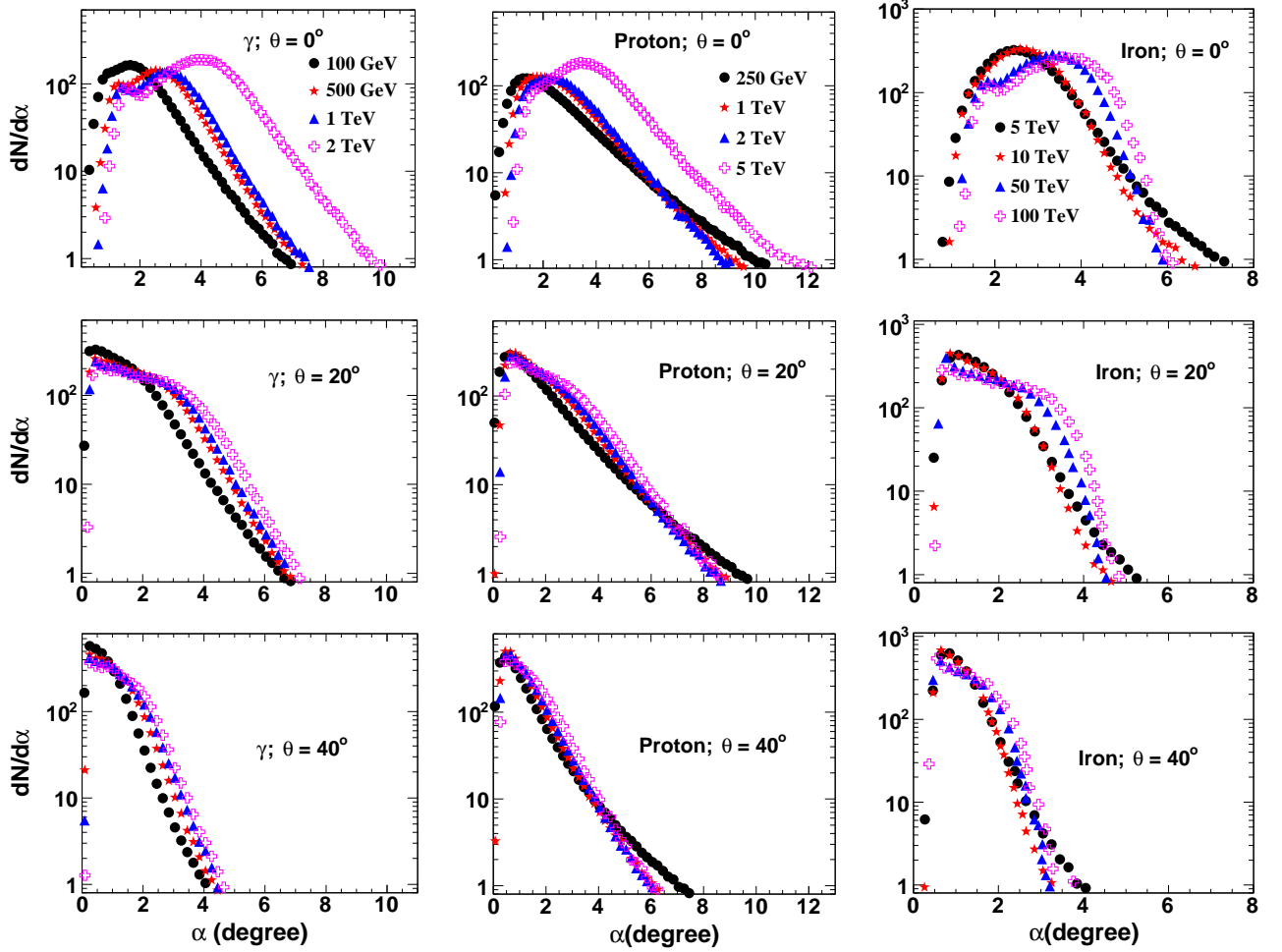


FIG. 17: Cherenkov photon's angular distributions obtained from different primaries with different energies corresponding to some fixed value of zenith angle of primary particle.

The Cherenkov photon's angular distributions that are obtained by using the EPOS-FLUKA and QGSJETII-FLUKA model combinations are shown in the Fig.19. It is observed that, there is hardly any difference between the results obtained from these two models for the γ -ray, proton and low energy iron primaries. However, for the iron primary at higher energy there is a slight difference between these two models' predictions, basically towards the higher side of the value of α . Higher the energy of the primary, more high energy secondary interactions, which results such differences in the distributions. It is also observed from this figure that apart from the position of maximum number of photons for the vertically incident shower, the distributions are almost similar for the same energy primaries of same type, incident at different zenith angles, specially for the case of γ -ray and proton primaries.

IV. SUMMARY AND CONCLUSION

Taking into consideration of the importance of effective techniques for the gamma hadron separation in ACT, we have made an effort here to study the Cherenkov photon's density, arrival time and angular distributions in EASs of vertically incident as well as inclined γ -ray, proton and iron primaries with different energies using the simulation package, the CORSIKA 6.990 [18]. This is the sequel of our earlier work [1] to generalize the study in extending energy and zenith angles of primary particles.

Cherenkov photon's density increases with energy for all primaries and decreases almost exponentially with increase in distance from the shower core. This is an obvious experimental fact that at a particular observation level it is easier to detect a high energy shower than a low energy shower and for a proper estimation of energy of a shower, the shower has to be well contained within the detector array. Also with increase in angle of inclination, the density decreases gradually near the shower core, but remains almost constant far away from the core. This result also supports the well known observational situation that, it is harder to detect an inclined than a vertical shower of same energy. γ -rays have the highest Cherenkov photon yield followed by proton and iron for any combination of energy, angle and hadronic interaction model. Thus, the equivalent energy of the iron primary must be highest followed by proton and γ -ray for a given Cherenkov photon yield for any cited combination.

The average arrival time of Cherenkov photon is found to increase according to an exponential function (see equation (3)) with increase in distance from the shower core for all combinations of energy and zenith angle. With increase in energy, the general trend shows an overall increase in the arrival time for all primaries. However, with the increasing zenith angle the arrival

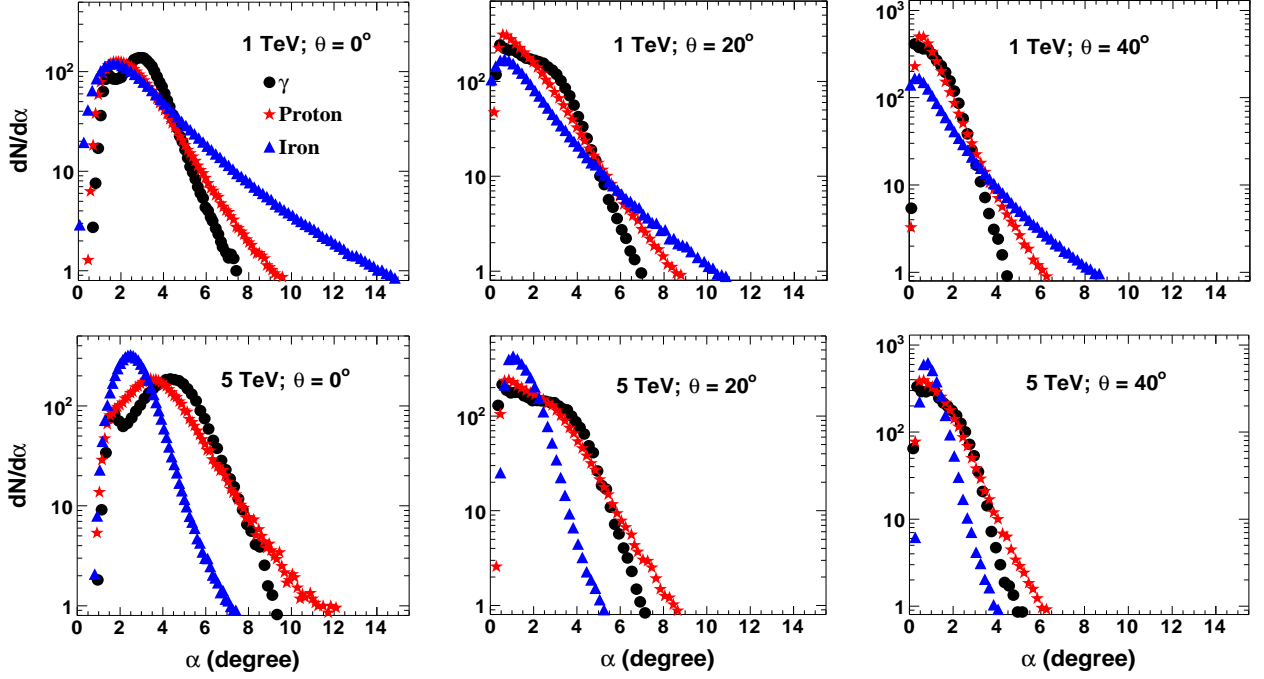


FIG. 18: Cherenkov photon's angular distributions obtained from different primaries with two different energies and zenith angles.

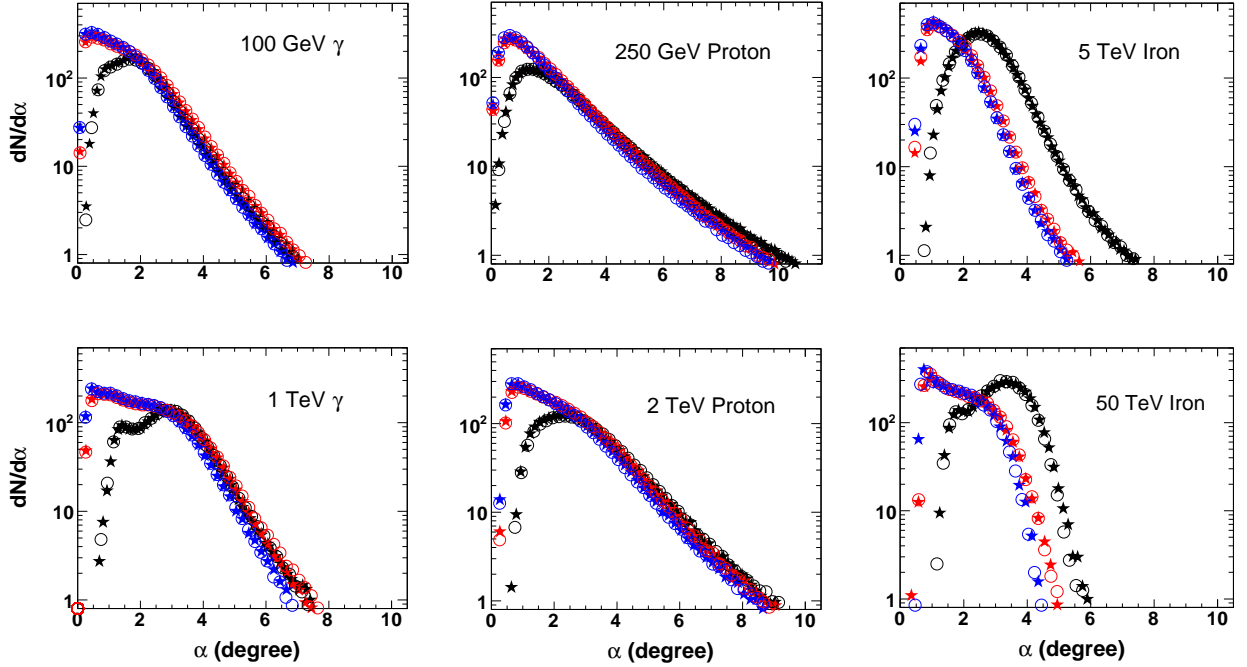


FIG. 19: Cherenkov photon's angular distributions for different primaries that are obtained by using the model combinations, viz., EPOS-FLUKA and QGSJETII-FLUKA. In the plots \star and \circ indicate the EPOS-FLUKA and QGSJETII-FLUKA respectively. Black colour represents 0° , red colour 10° and blue colour 20° zenith angle of the primary particle.

time profile becomes flatter and hence there is a decrease in arrival time. At a particular energy and an angle of incidence, the average arrival time is highest for the γ -ray primary and least for the iron primary. All these information along with the features of density distribution may be useful to disentangle the showers of γ -ray from the hadronic showers while analyzing the experimental EAS data, apart from usual determination of direction of a shower from the arrival time information.

In general, the shower to shower fluctuation for density and arrival time of Cherenkov photons decreases with increasing energy of primary particle, and is highest for proton primary and least for the γ -ray primary at all zenith angle. While estimating the systematic uncertainties in the data of a γ -ray experiment, this information will provide an important input to be considered.

As we have seen in our earlier work [1], the density of photons increases with increasing altitude of observation level for all primaries, but decreases with the increasing zenith angle of all these particles. At highest zenith angle (40°) the characteristic hump is also seen for the iron primary at lower altitude of the observation level. Similarly, the Cherenkov light front is flatter

for the lower observation altitude as well as for the larger zenith angle of all primary particles. Thus the recording time of an inclined shower for a γ -ray telescope array at a lower observation level is less than that for a vertical shower of same energy and observed at higher observation level.

In the calculation of density and arrival time distributions of Cherenkov photons, on average four different atmospheric models (viz., U.S. standard atmosphere as parameterized by Linsley, AT 115 Central European atmosphere for Jan. 15, 1993, Malargüe winter atmosphere I after Keilhauer and U.S. standard atmosphere as parameterized by Keilhauer) available in the CORSIKA give almost similar results. Thus this analysis shows that any one of them may be used within a reasonable limit of error.

The angular distributions of Cherenkov photons have distinct features in connection with the type of primary particle, its energy and zenith angle. For vertical showers of all primaries, the Cherenkov photon's angular position with respect to shower axis at which maximum photons are concentrated shifts to higher value with increasing energy of the primary. This tendency is highest for the γ -ray primary and least for the iron primary. With increasing zenith angle, the maximum photons are found to be remained within very near to the shower axes for all energy primaries. Also distributions for all primaries and energies gradually become narrower with increasing zenith angle. At low energy the iron primary has largest angular distribution at all zenith angles, whereas at higher energy it is the proton which has the largest distribution.

Moreover, the QGSJETII-FLUKA and EPOS-FLUKA model combinations produce almost similar results in the density, arrival time and angular distributions. So, any of these two high energy models can be used to analyze the experimental data of γ -ray astronomy.

A clear understanding of Cherenkov photon's density, arrival time and angular distributions for different primary particle with different energy and at different zenith angle, and also their possible interdependence will be greatly helpful to develop a more efficient technique of gamma-hadron separation in future. In this context a full parameterizations study on these sensitive parameters is very essential. We hope to report such work in future as a part of complete simulation study on atmospheric Cherenkov photons.

Acknowledgments

We are thankful to anonymous referees for their useful comments, which leads to further improve the work. UGD is thankful to the Inter-University Centre for Astronomy and Astrophysics (IUCAA), Pune for hospitality during his visit as a Visiting Associate.

-
- [1] P. Hazarika, U. D. Goswami, V. R. Chitnis, B. S. Acharya, G. S. Das, B. B. Singh, R. Britto, *Astropart. Phys.* **68**, 16 (2015) [arXiv:1404.2068].
 - [2] René A. Ong, *Phys. Reports* **305**, 93 (1998).
 - [3] C. M. Hoffman and C. Sinnis, *Rev. Mod. Phys.* **71**, 897 (1999).
 - [4] T. C. Weekes, *astro-ph/0811.1197v1* (2009).
 - [5] E. Lorenz and R. Wagner, *EPJ H* **37**, 459 (2012) [arXiv:1207.6003].
 - [6] J. Holder, *Braz. J. Phys.* **44**, 450 (2014) [arXiv:1407.1080].
 - [7] S. Funk, *Annu. Rev. Nucl. Part. Sci.* **65**, 245 (2015).
 - [8] B. Degrange and G. Fontaine, *C. R. Physique* **16**, 587 (2015) [arXiv:1604.05488].
 - [9] M. Lemoine-Goumard, arXiv:1510.01373 (2015).
 - [10] P. N. Bhat, *Bull. Astr. Soc. India* **30**, 135 (2002).
 - [11] B. S. Acharya, 29th ICRC, **10**, 271 (2005).
 - [12] J. Holder, arXiv:1510.05675 (2015).
 - [13] H. M. Bardan, T. C. Weekes, *Astropart. Phys.* **7**, 307 (1997); Herve Cabot et al., *Astropart. Phys.* **9**, 269 (1998).
 - [14] V. R. Chitnis, P. N. Bhatt, *Astropart. Phys.* **15**, 29 (2001).
 - [15] A. M. Hillas, *J. Phys. G: Nucl. Phys.* **8**, 1461 (1982).
 - [16] S. Lafebre, R. Engel, H. Flacke, J. Horandel, T. Huege, J. Kuijpers, R. Ulrich, *Astropart. Phys.* **31**, 243 (2009).
 - [17] F. Nerling, J. Blumer, R. Engel, M. Risse, *Astropart. Phys.* **24**, 421 (2006).
 - [18] J. Knapp, D. Heck, *EAS Simulation with CORSIKA V 6990: A User's Guide* (1998); D. Heck et al., Report **FZKA 6019** (1998), Forschungszentrum Karlsruhe; http://www.wik.fzk.de/corsika/physicsdescription/corsika_phys.html
 - [19] W. R. Nelson, H. Hirayama, D. W. O. Rogers, *The EGS4 Code System*, SLAC Report 265 (1985).
 - [20] U. D. Goswami, *Astropart. Phys.* **28**, 251 (2007).
 - [21] T. Pierog, K. Werner, *Nucl. Phys. Proc. Suppl.* **196**, 102 (2009) [arXiv:0905.1198].
 - [22] US Standard Atmosphere (US Govt. Printing Office, Washington, 1962).
 - [23] <http://root.cern.ch>
 - [24] U. D. Goswami, K. Boruah, P. K. Boruah, T. Bezboruah, *Astropart. Phys.* **22**, 421 (2005).